Aperture–Bandwidth Characteristics of the Acousto-Optic Filter*

S. T. K. NIEH AND S. E. HARRIS
Microwave Laboratory, Stanford University, Stanford, California 94305
(Received 15 September 1971)

A theoretical and experimental study of the aperture–bandwidth characteristics of the electronically tunable acousto-optic filter shows that (a) optical divergence in the ordinary plane of the acousto-optic crystal results in a broadening of the filter frequency-transmission characteristic toward longer wavelengths; (b) optical divergence in the extraordinary plane results in a broadening toward shorter wavelengths; (c) divergence of the acoustic beam has the same effect as optical ordinary divergence, and generally will not be of consequence; and (d) roughly, the resolution times the solid-angle acceptance of the acousto-optic filter is approximately the same as that of a solid Fabry–Perot interferometer made of the same material.
INDEX HEADINGS: Filters; Crystals; Polarization.

In this paper, we report a study of the effect of angular divergence on the shape of the transmittance vs frequency characteristic of the electronically tunable acousto-optic filter. As noted in earlier papers,[1–3] this filter operates by allowing an acoustic wave and a linearly polarized optical wave to propagate collinearly in an appropriate optically anisotropic crystal. The crystal orientation is chosen so that on a microscopic basis, any incident optical frequency is diffracted or scattered into the orthogonal polarization.[4] For this scattering to be cumulative over the length of the crystal, it is necessary that the ordinary optical wave, the extraordinary optical wave, and the acoustic wave be **k**-vector matched. At a given acoustic frequency only a small band of optical frequencies is cumulatively diffracted and transmitted through the orthogonal output polarizer. By changing the incident acoustic frequency, we may tune the filter over broad regions of the uv, visible, or ir spectrum.

To date, we have studied two basic versions of this filter. These are a reflection-type $LiNbO_3$ filter[2] and a transmission-type $CaMoO_4$ filter.[3] The $LiNbO_3$ filter had a measured half-power bandpass <2 Å and a theoretically estimated bandpass of 1.76 Å. The $CaMoO_4$ had a measured bandpass of 8 Å. Maximum transmittances, corrected for optical reflection losses, of these filters for linearly polarized light were 50 and 94%, respectively. Both were tunable from about 5000 to 7000 Å; this range of tuning was limited by the bandwidth of the acoustic transducers. A schematic of the transmission-type $CaMoO_4$ filter, along with its tuning curve, is shown in Fig. 1.

ANALYSIS OF ANGULAR CHARACTERISTICS

It is immediately clear that angular divergence or deviation of either the incident optical beam or of the incident acoustic beam affects the **k**-vector-matching condition and thus will result in a broadening or skewing of the filter-transmittance characteristic.

For definiteness and in order to compare the results with experiment, we consider the case of a transmission-type $CaMoO_4$ filter. The analysis proceeds very similarly to that of Ref. 1, except that now we explicitly allow for paraxial rays. Because the efficiency of an acousto-optic interaction varies as the sixth power of the optical refractive index, materials used for this type of interaction often have an index greater than two. External angles are thus magnified over internal angles by two or more, making the analysis valid for external half-angles of about 0.2 radians or f/numbers of about 2.5.

The applied acoustic wave is an S_4 shear wave polarized along the z axis. The input and output optical waves are polarized along the z and x axes, respectively. Thus,

$$\hat{E}_z(\mathbf{r},t)=\frac{E_z(\mathbf{r})}{2}\exp j(\omega_e t-\mathbf{k}_e\cdot\mathbf{r})+\text{complex conjugate},$$
$$\hat{E}_x(\mathbf{r},t)=\frac{E_x(\mathbf{r})}{2}\exp j(\omega_0 t-\mathbf{k}_0\cdot\mathbf{r})+\text{complex conjugate},\quad(1)$$
$$\hat{S}_4(\mathbf{r},t)=\frac{S_4}{2}\exp j(\omega_a t-\mathbf{k}_a\cdot\mathbf{r})+\text{complex conjugate},$$

where ω_e, ω_0, ω_a and $\mathbf{k}_e$, $\mathbf{k}_0$, and $\mathbf{k}_a$ are the frequencies and **k** vectors of the three interacting waves. $E_z(\mathbf{r})$ and $E_x(\mathbf{r})$ are slowly varying envelope quantities and S_4 is assumed to be independent of **r**.

Utilizing the photoelastic tensor for $CaMoO_4$ (point group $4/m$) and substituting into Maxwell's equations, we obtain the coupled equations

$$\frac{\mathbf{k}_0}{|\mathbf{k}_0|}\cdot\nabla\mathbf{E}_x(\mathbf{r})=j\frac{\omega_0 n_0 n_e^2 p_{45} S_4^*}{4c}E_z(\mathbf{r})e^{-j\Delta\mathbf{k}\cdot\mathbf{r}},$$
$$\frac{\mathbf{k}_e}{|\mathbf{k}_e|}\cdot\nabla\mathbf{E}_z(\mathbf{r})=j\frac{\omega_e n_e n_0^2 p_{45} S_4}{4c}E_x(\mathbf{r})e^{j\Delta\mathbf{k}\cdot\mathbf{r}},\quad(2)$$
$$\Delta\mathbf{k}=\mathbf{k}_e-\mathbf{k}_0-\mathbf{k}_a,$$

where p_{45} is the pertinent photoelastic coefficient, n_0 and n_e are the ordinary and extraordinary refractive indices, and c is the velocity of light in free space.

We now assume the incident optical beam to be polarized in the extraordinary plane and to have **k** vector $\mathbf{k}_e$. The magnitudes of $\mathbf{k}_e$ and $\mathbf{k}_0$ and the direction of $\mathbf{k}_e$ are thus assumed, whereas the direction of $\mathbf{k}_0$ is

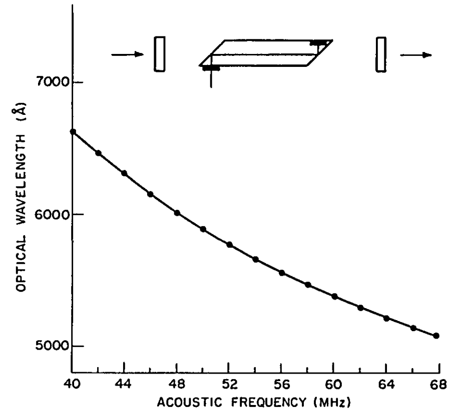

FIG. 1. Schematic of electronically tunable optical filter and tuning curve for a $CaMoO_4$ filter. The acoustic wave is brought in via the transducer at the lower left corner of the $CaMoO_4$ crystal; is reflected off the $CaMoO_4$ air interface; and after traveling down the length of the $CaMoO_4$ crystal is terminated in an aluminum and wax termination.

to be determined. [Note that the relations $|\mathbf{k}_0|=\omega n_0/c$ and $|\mathbf{k}_e|=\omega n_e/c$ are implicit in Eq. (2).]

To determine the direction of $\mathbf{k}_0$, we follow Kleinman[5] and choose $\mathbf{k}_0$ such that its tangential component along the boundary $y=0$ equals the tangential component of its driving-polarization wave vector $\mathbf{k}_e—\mathbf{k}_a$. This ensures that the boundary is a constant-phase surface and also results in a k-vector mismatch $\mathbf{\Delta k}$ that is orthogonal to the boundary. Using the construction and coordinate system of Fig. 2, we obtain from Eq. (2)

$$\frac{\partial E_x}{\partial \xi'}=j\frac{\omega_0 n_0 n_e^2 p_{45} S_4^*}{4c}E_z e^{-j\Delta k y}, \quad (3a)$$

$$\frac{\partial E_z}{\partial \xi''}=j\frac{\omega_e n_e n_0^2 p_{45} S_4}{4c}E_x e^{j\Delta k y}, \quad (3b)$$

where

$$\mathbf{\Delta k}=\Delta k \mathbf{a}_y$$

and

$$\Delta k=\frac{2\pi n_e}{\lambda_0}-\frac{2\pi n_0}{\lambda_0}-\frac{2\pi f_a}{V_a}+\frac{\pi\lambda_0}{n_0}\left(\frac{n_e\theta_e}{\lambda_0}-\frac{f_a\theta_a}{V_a}\right)^2+\frac{\pi\lambda_0}{n_0}\left(\frac{n_e\varphi_e}{\lambda_0}-\frac{f_a\varphi_a}{V_a}\right)^2-\frac{\pi n_e}{\lambda_0}\left(\frac{n_e^2}{n_0^2}\theta_e^2+\varphi_e^2\right)+\frac{\pi f_a}{V_a}(\theta_a^2+\varphi_a^2), \quad (4)$$

where f_a and V_a are the acoustic frequency and velocity, respectively, and we have assumed small-angle variation for the extraordinary index n_e. We also note that we have neglected the inconsequential frequency shift f_a/f_0 that is introduced by the acousto-optic interaction. The variables ξ' and ξ'' in Eqs. (3a) and (3b) are the length variables measured in the direction of travel of the ordinary and extraordinary waves, respectively. Because $|\mathbf{k}_a|\ll|\mathbf{k}_0|$ or $|\mathbf{k}_e|$, we take $\xi''=\xi'$ equal to a mean variable $\xi=y/\cos\gamma$, where γ is the relative angle between the input beam (internal to the crystal) and the y axis. We thus obtain

$$\frac{\partial E_x}{\partial \xi}=j\frac{\omega_0 n_0 n_e^2 p_{45} S_4^*}{4c}E_z e^{-j\Delta k\xi\cos\gamma},$$
$$\frac{\partial E_z}{\partial \xi}=j\frac{\omega_e n_e n_0^2 p_{45} S_4}{4c}E_x e^{+j\Delta k\xi\cos\gamma}. \quad (5)$$

Because we are interested in the angular-frequency characteristic of the filter in the vicinity of some central optical wavelength, to which it is tuned, we set

$$\frac{2\pi n_e}{\lambda_0}-\frac{2\pi n_0}{\lambda_0}-\frac{2\pi f_a}{V_a}=0$$

in Eq. (4) and write the frequency-dependent portion of Δk as

$$\Delta k=\left(\frac{\partial k_e}{\partial y}-\frac{\partial k_0}{\partial y}\right)\Delta y$$
$$=b\Delta y, \quad (6)$$

where Δy is the excursion measured in cm^{-1} from the optical center wavelength λ_0. Figure 3 gives the dispersive constant b, based on the refractive index data of Bond,[6] for $CaMoO_4$.

To the accuracy of the present analysis we may set $\cos\gamma=1$ in Eq. (5) and readily solve the resulting

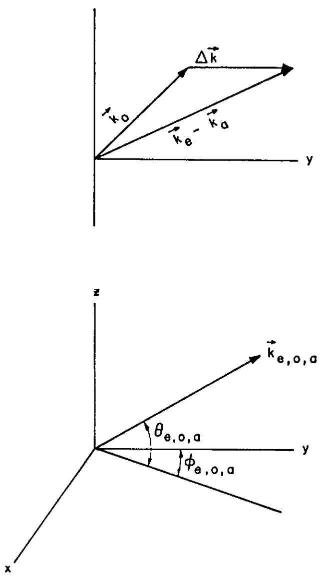

FIG. 2. Construction for the determination of the k-vector mismatch $\mathbf{\Delta k}$ and angular coordinates for analysis. In the upper portion of this figure, the vector $\mathbf{k}_e-\mathbf{k}_a$ denotes the acoustic driving polarization, while the vector $\mathbf{k}_0$ denotes the three electromagnetic waves.

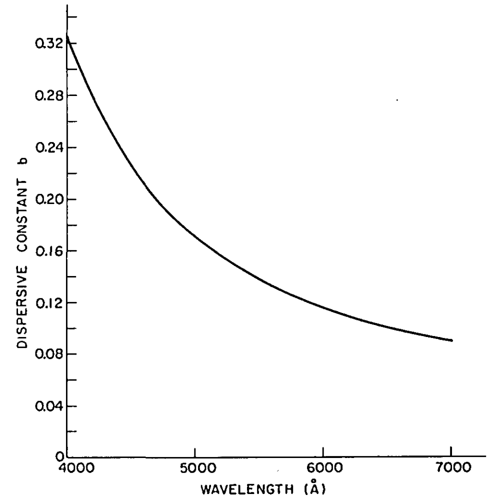

FIG. 3. Dispersive constant b vs wavelength for $CaMoO_4$.

coupled equations. Evaluating at the output of the crystal $\xi=L$, we obtain the angular wavelength-transfer function of the filter

$$H(\Delta y,\theta_e,\varphi_e,\theta_a,\varphi_a)=\Gamma^2L^2\frac{\sin^2(\Gamma^2L^2+\Delta k^2L^2/4)^{\frac{1}{2}}}{\Gamma^2L^2+\frac{1}{4}\Delta k^2L^2}, \quad (7)$$

where

$$\Gamma^2=\frac{n_0{}^3n_e{}^3p_{45}{}^2\pi^2}{4\lambda_0{}^2}|S_4|^2$$

$$=\frac{n_0{}^3n_e{}^3p_{45}{}^2\pi^2}{2\rho V_a{}^3\lambda_0{}^2}\left(\frac{P_A}{A}\right)$$

and

$$\Delta k=\frac{\pi\lambda_0}{n_0}\left(\frac{n_e\theta_e}{\lambda_0}-\frac{f_a\theta_a}{V_a}\right)^2+\frac{\pi\lambda_0}{n_0}\left(\frac{n_e\varphi_e}{\lambda_0}-\frac{f_a\varphi_a}{V_a}\right)^2$$
$$-\frac{\pi n_e}{\lambda_0}\left(\frac{n_e{}^2}{n_0{}^2}\theta_e{}^2+\varphi_e{}^2\right)+\frac{\pi f_a}{V_a}(\theta_a{}^2+\varphi_a{}^2)+b\Delta y, \quad (8)$$

where P_A/A is the acoustic power density and ρ is the mass density. For $CaMoO_4$ at 5000 Å, $\Gamma^2\cong 5.2\times 10^{-3}(P_A/A)$ cm^{-2}, where we have used our measured value $p_{45}\cong 0.068$ and P_A/A has units of mW/mm^2.

More generally, for incident optical power distributions of the form $I(\Delta y,\theta_e,\varphi_e)$, the transmitted power distribution is given by

$$T(\Delta y)=\int_{\theta_e,\varphi_e,\theta_a,\varphi_a} H(\Delta y,\theta_e,\varphi_e,\theta_a,\varphi_a)\times I(\Delta y,\theta_e,\varphi_e)\,d\theta_e\,d\varphi_e\,d\theta_a\,d\varphi_a \Big/ \int_{\theta_e,\varphi_e,\theta_a,\varphi_a} I(\Delta y,\theta_e,\varphi_e)\,d\theta_e\,d\varphi_e\,d\theta_a\,d\varphi_a. \quad (9)$$

EFFECT OF OPTICAL AND ACOUSTIC DIVERGENCE

We start by noting separately the effects of different types of divergence.

(*i*) *Optical divergence in the* x, y *(ordinary) plane* ($\theta_a=\varphi_a=0$; $\theta_e=0$). From Eq. (8), we obtain

$$\Delta k=\frac{\pi n_e(n_e-n_0)}{n_0\lambda_0}\varphi_e{}^2+b\Delta y. \quad (10)$$

Because b is a positive constant, finite divergence or misalignment in the x, y plane broadens or shifts the transmission band of the filter toward longer wavelengths.

Figures 4(a) and 4(b) show optical transmittance vs wavelength deviation for a 5-cm-long $CaMoO_4$ filter centered at 5000 Å. Figure 4(a) assumes that the acoustic and optical beams are perfectly collimated and travel down the y axis of the crystal. Figure 4(b) assumes uniform optical divergence in the ordinary plane. To obtain this figure $I(\Delta y,\varphi_e)$ was assumed constant between $\varphi_e=-0.035$ and 0.035 radians. For all parts of Fig. 4 the acoustic drive level was assumed set at $\Gamma L=\pi/4$, thus yielding 50% transmittance for a perfectly collimated input beam. We note that the effect of optical divergence is to skew the wavelength response toward longer wavelengths and also to reduce the peak transmittance from 50%. This reduction of transmittance results because off-axis rays are not transmitted at the same amplitude as is a collinear ray.

(*ii*) *Optical divergence in the* y, z *(extraordinary) plane* ($\theta_a=\varphi_a=0$; $\varphi_e=0$). From Eq. (8), we obtain

$$\Delta k=-\frac{\pi n_e{}^2(n_e-n_0)}{n_0{}^2\lambda_0}\theta_e{}^2+b\Delta y. \quad (11)$$

In this case finite divergence or misalignment broadens or shifts the transmission characteristics to shorter wavelengths.

Figure 4(c) shows optical transmittance vs frequency for an optical beam having a uniform divergence in the y, z plane from $\theta_e=-0.035$ radians to $\theta_e=+0.035$ radians.

(*iii*) *Combined ordinary and extraordinary divergence* ($\theta_a=\varphi_a=0$). From Eqs. (10) and (11) we see that the constants that determine the broadening in the x, y and y, z directions are approximately equal, and thus a symmetrically uniformly divergent optical beam will broaden the transmission characteristics nearly equally in the short- and the long-wavelength directions.

Figure 4(d) shows transmittance vs frequency for an optical beam uniformly divergent over the range $\varphi_e=\theta_e=-0.035$ radians to $\varphi_e=\theta_e=+0.035$ radians.

(*iv*) *Acoustic divergence* ($\theta_e=\varphi_e=0$). From Eq. (8), we obtain

$$\Delta k=\frac{\pi n_e(n_e-n_0)}{n_0\lambda_0}(\theta_a{}^2+\varphi_a{}^2)+b\Delta y. \quad (12)$$

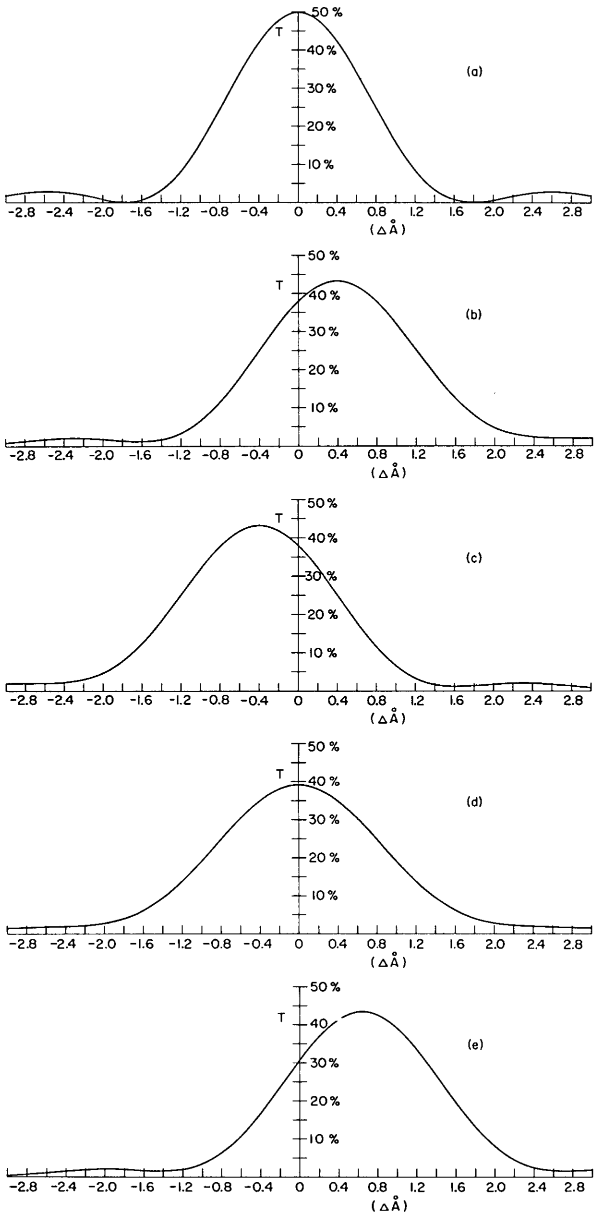

FIG. 4. Filter transmittance versus optical wavelength deviation (ΔÅ) from 5000 Å. The figure assumes a 5-cm $CaMoO_4$ crystal and notes the effect of different types of optical divergence as follows: (a) no divergence; (b) optical ordinary divergence; (c) optical extraordinary divergence; (d) both ordinary and extraordinary optical divergence; and (e) acoustic divergence. All cases except (a) assume a uniformly diverging beam of half-angle internal divergence varying between -0.035 radians and $+0.035$ radians.

From Eqs. (10) and (12) we see that divergence of the acoustic beam has the same effect as optical ordinary divergence.

Figure 4(e) shows transmittance vs frequency for a perfectly collimated optical beam and an acoustic beam with an assumed maximum half-angle divergence of 0.035 radians. For reference, we note that the acoustic divergence produced by diffraction from a transducer

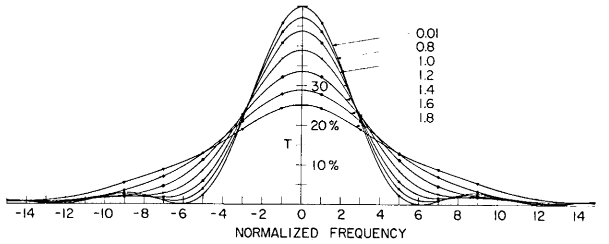

FIG. 5. Filter transmission curves as a function of parameter $(\Delta nL/\lambda_0)^{\frac{1}{2}}\psi$ and normalized frequency $bL\Delta y$.

3 mm in diameter at an acoustic frequency of 50 MHz is 0.02 radians. Since we expect that transducers will typically be at least this large, acoustic divergence will not usually be of consequence.

NORMALIZED-FREQUENCY ANGULAR RESPONSE

For uniform conical optical divergence in the ordinary and extraordinary planes, we may define a parameter $(\Delta nL/\lambda_0)^{\frac{1}{2}}\psi$, where $\psi=\theta_{e\max}=\varphi_{e\max}$. Figure 5 shows a set of normalized filter-transmittance characteristics for uniform conical optical divergence. These curves are applicable to filters centered at any wavelength and of different crystal lengths. As previously, the acoustic drive level was adjusted so as to provide 50% transmittance at band center for perfectly collimated incident light. From these curves, we see that an optical divergence less than about $(\Delta nL/\lambda_0)^{\frac{1}{2}}\psi=0.8$ has little effect on the transmittance characteristic.

Figure 6 shows the percentage broadening of half-power bandwidth of the filter vs the parameter $(\Delta nL/\lambda_0)^{\frac{1}{2}}\psi$. The curve breaks at approximately $\psi=(\lambda_0/\Delta nL)^{\frac{1}{2}}$, at which the external solid acceptance angle is

$$\Omega=n_e n_0 \pi\psi^2=\frac{n_e n_0 \pi\lambda_0}{\Delta nL}. \qquad (13)$$

From Eq. (7) we see that for an acoustic drive strength of $\Gamma L=\pi/4$ (50% transmittance for collimated

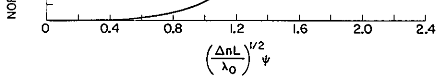

FIG. 6. Normalized half-power bandwidth vs normalized angular divergence. The angularly broadened bandwidth is normalized to the half-power bandwidth in the absence of angular broadening. ψ is the internal half-angle divergence.

light), the half-power filter bandwidth is approximately $5/bL$, which for crystals of typical dispersion is about $1/2\Delta nL$. Thus for typical dispersion, the acousto-optic filter in nearly collimated light has a spectral resolution

$$R=\frac{\lambda}{\Delta\lambda}=\frac{2\Delta nL}{\lambda_0}.$$

Combining this with Eq. (13), we have

$$R\Omega=n_e n_0 2\pi. \tag{14}$$

The product of the resolution and the solid acceptance angle of the acousto-optic filter is about $n^2 2\pi$, and is thus about the same as a Fabry–Perot interferometer made of the same material. The tunable filter has the important advantage of a free-spectral range that is in principle equal to the entire wavelength region over which the crystal is transparent.

EXPERIMENTAL RESULTS

A transmission-type filter was constructed to check the preceding analysis. This filter has been described previously and is shown in Fig. 7. The acoustic shear wave was generated in the $CaMoO_4$ crystal by a $LiNbO_3$ acoustic transducer and was reflected at a 45° interface to travel collinearly with the light. Since the $CaMoO_4$ air interface has a critical angle of 30°, an optical-index-matching oil was used to bring the light wave into the crystal. A relatively short crystal ($L=1.8$ cm) and an acoustic transducer of fairly large area (4 mm by 5 mm) were used to accommodate large angular apertures. The acoustic transducer was 144 μm thick and was operated at its third harmonic resonance.

The angular divergence of the incident light was controlled by a variable aperture placed in the front focal plane of a collimating lens that preceded the filter. Because of the 45°-cut input interface, the symmetrically diverging beam outside the crystal becomes elliptically diverging inside the crystal. As shown by Fig. 7, rays diverging in the ordinary plane are refracted more than rays diverging in the extraordinary plane. Thus, inside the crystal, angular divergence in the ordinary plane is smaller. We therefore expect some skewing toward shorter wavelengths. After passing through the filter, the transmitted light was focused onto the entrance slit of a Spex monochromator having a resolution of about 0.5 Å.

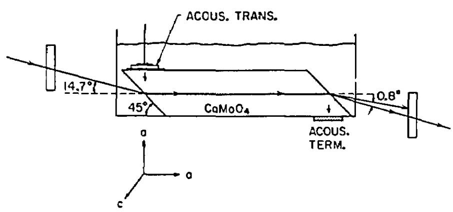

FIG. 7. Schematic of $CaMoO_4$ transmission-type acousto-optic filter.

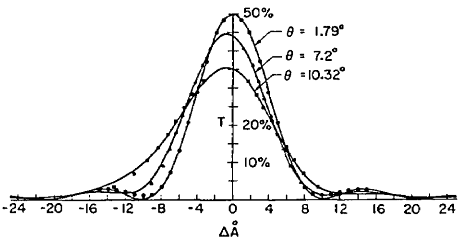

FIG. 8. Experimental and theoretical comparison of filter transmission for uniformly diverging optical beams with different maximum angular aperture. The $CaMoO_4$ crystal was 1.8 cm long and centered at 5940 Å. In this figure, θ is the maximum external half-angle.

Figure 8 shows experimental and theoretical results for three different angular apertures. In each case the acoustic drive level was set for 50% transmittance for a collimated light beam. In calculating the theoretical curve, account was taken of the above-mentioned asymmetry of internal angles. As shown by the figure, the experimental check was quite good.

CONCLUSIONS

The paper has presented formulas and curves for the angular aperture of the acousto-optic filter. Principal results are (a) optical divergence in the ordinary plane results in a broadening of the filter transmission toward longer wavelengths; (b) optical divergence in the extraordinary plane results in broadening toward shorter wavelengths; (c) acoustic divergence has the same effect as optical divergence in the ordinary plane and typically will not be of consequence; and (d) roughly, the resolution times the solid angle of acceptance of the acousto-optic filter is the same as that of a solid Fabry–Perot interferometer made of the same material.

ACKNOWLEDGMENTS

The authors acknowledge helpful discussions with Dr. Pinard, Dr. Young, and Dr. Kuizenga. We thank R. Griffin and F. Futtere for assistance in constructing the acoustic transducers and R. Feigelson and Wayne Kway of the Stanford Center for Materials Research for growing the $CaMoO_4$ crystals.

REFERENCES

* The work reported in this paper was sponsored jointly by the Office of Naval Research under Contract N00014-67-A-0112-0036 and by the Joint Services Electronics Program through the Office of Naval Research.
[1] S. E. Harris and R. W. Wallace, J. Opt. Soc. Am. **59**, 744 (1969).
[2] S. E. Harris, S. T. K. Nieh, and D. K. Winslow, Appl. Phys. Letters **15**, 325 (1969).
[3] S. E. Harris, S. T. K. Nieh, and R. S. Feigelson, Appl. Phys. Letters **17**, 223 (1970).
[4] R. W. Dixon, IEEE J. **QE-3**, 85 (1967).
[5] D. A. Kleinman, A. Ashkin, and G. D. Boyd, Phys. Rev. **145**, 338 (1966).
[6] W. L. Bond, J. Appl. Phys. **36**, 1674 (1965).